This is the authors' accepted manuscript of a paper published in Proceedings of 11th International Conference on Electrical, Electronics and Computer Engineering (IcETRAN), Nis, 3-6 June 2024
The final version of record is available via IEEE Xplore

Solar Charger for Mobile Applications

Lazar Lukić
School of Electrical Engineering
University of Belgrade
Belgrade, Serbia
ll233064m@student.etf.bg.ac.rs

Milovan Majstorović
School of Electrical Engineering
University of Belgrade
Belgrade, Serbia
majstorovic@etf.bg.ac.rs

Leposava Ristić
School of Electrical Engineering
University of Belgrade
Belgrade, Serbia
leposava.ristic@etf.bg.ac.rs

Francisco de Paula Garcia Lopez
Department of Electrical Engineering
University of Seville
Seville, Spain
fdpgarcia@us.es

***Abstract*—The paper presents off-grid DC system which contains photovoltaic panel, cascaded buck-boost converter and lithium-ion battery. It addresses the problem of charging battery with wide range of input voltages depending on type of photovoltaic panel and weather conditions. The converter topology is proposed and the control algorithm is developed. Control in the loop test is provided at the laboratory setup. The test results prove the concept of the proposed system with simple design and great flexibility of input voltage acquired from photovoltaic panel to output voltage, required from battery.**

Keywords— Photovoltaic panel, Cascaded Buck-Boost Converter, Lithium-ion Battery, Hysteresis control

I. INTRODUCTION

In order to reduce pollution and preserve fossil fuels many efforts have been made to enable so called clean electrical energy production. With the rapid increase in energy consumption, the production and storage of solar energy from renewable energy sources has become an important subject [1]. With the use of renewables which are intermittent and variable energy sources like photovoltaic (PV) panel and wind, the requirement of storing energy and then deploying it in the case of interrupted power supply due to shortages is becoming common [2]. Power electronics is crucial when it comes to implementation of renewable power sources in grid-connected power systems as well as off-grid systems. Although grid-connected renewables are of great importance for future concept and design of power system, focus of this paper relies on application of PV in off-grid systems. It is convenient to have power sources (that do not require external refill) on inaccessible places. Semiconductor era and rising development of power electronics enabled it.

The main idea behind this paper was to investigate the possibility of constructing universal solar charger which would charge battery from wide range of PV panel types combined with wide range of weather conditions. The level of irradiation affects PV panel short circuit current (I_{SC}), while ambient temperature has impact on PV panel open circuit voltage (V_{OC}) [3]. Depending on values of I_{SC} and V_{OC} developed solar charger algorithm decides which one of multiple charging modes should be active.

The difference between charging modes arises from different states of charge of the battery and depends on level of irradiation. Although charging should be as fast as possible, charging time cannot be arbitrarily short. In order to prevent battery damage, charging current must be maintained bellow predefined value. Nearly full battery is extremely vulnerable if high charging current is supplied.

The rest of the paper is organized as follows: the topology of the proposed converter is firstly presented, followed by the control implementation and results of Hardware in the Loop (HIL) testing. Accordingly, adequate conclusions are derived with plans for future work.

II. CONVERTER TOPOLOGY

Aforementioned cascaded buck-boost (CBB) converter whose topology is shown in Fig. 1 and in [4-7], is proposed in the paper due to its simple design and universality in terms of adjustment of supplied input voltage (V_{PV}) to output voltage (V_{BATT}) whether V_{PV} is lower or higher than V_{BATT}. The application of buck (*boost*) converter eliminates possibility to charge battery with input voltage that is lower (*higher*) than battery voltage.

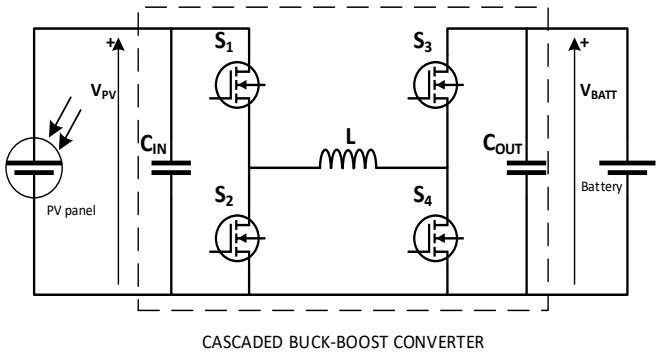

Fig. 1 System under the test: Photovoltaic panel (left), Cascaded buck-boost converter (middle) and Battery (right)

The developed algorithm as inputs uses: battery voltage (V_{BATT}), battery current (I_{BATT}), PV panel voltage (V_{PV}), PV panel current (I_{PV}). As outputs, algorithm provides duty cycles for converter switches. Targeted switches (Fig. 1) are upper switch in the first leg (S_1) and lower switch in the second leg (S_4). When the converter is required to operate as buck, duty cycle D_1 for switch S_1 varies and duty cycle D_4 for switch S_4 is zero. When the converter is required to operate as boost, duty cycle D_1 for

switch S_1 is one and duty cycle D_4 for switch S_4 varies. If it is assumed that dead time could be neglected, following relations for duty cycles are: $D_1+D_2=1$ and $D_3+D_4=1$.

For better illustration of the proposed converter operation, switching states are shown in Fig. 2 (a, b, c, d). Current flow is demonstrated with dashed red line. Light grey color represents switches which are inactive for shown switching state. CBB is actually used as synchronous buck converter in buck mode, and in boost mode CBB is used as synchronous boost converter, based on Fig. 2.

III. Implemented Control

Based on whether the PV panel voltage is higher or lower than the battery voltage, it is determined which one of buck or boost mode of converter operation is active. For each of two previously mentioned modes there are three different ways of charging battery: CC mode (Constant Current), CV mode (Constant Voltage) and MPPT mode (Maximum Power Point Tracking). The CC mode is supposed to be active for most of the charging time and implies battery charging with maximum possible current (current limit) that does not endangers the battery itself. When the battery is nearly full and its voltage is around maximum level, CV mode is desirable. It maintains battery voltage level on nearly constant level and provides charging with low current. High currents can harm nearly full battery and decrease its life span. The MPPT mode is active whenever conditions for CC or CV mode are not met. For example, when irradiation is low and it is not possible to reach and maintain current limit for CC mode, active mode should be MPPT mode which provides charging with maximum power. But, when irradiation is so high that charging with maximum power implies battery current that is over current limit, active mode should be CC mode which maintains current bellow that limit.

General algorithm flowchart is shown in Fig. 3. Only difference between buck and boost mode is which one of two duty cycles, D_1 or D_4, is incremented or decremented. Basic input/output current and input/output voltage relations for buck converter also stand for CBB buck mode, as well as basic relations for boost converter, that-also stand for CBB boost mode [8]. Throughout the paper following form will be used.

Buck converter: $$I_{PV} = I_{BATT} \cdot D,\ V_{PV} = \frac{V_{BATT}}{D}. \quad (1)$$

Boost converter: $$I_{PV} = \frac{I_{BATT}}{1-D},\ V_{PV} = V_{BATT} \cdot (1-D). \quad (2)$$

Note that increment (*decrement*) of duty cycle in previous relations results in rise (*fall*) of input currents, so as in fall (*rise*) of input voltages. Hence, varying of duty cycle affects the input currents and voltages in the same manner for both buck and boost mode.

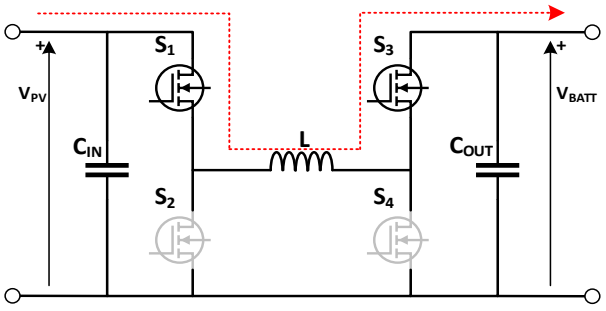

Fig. 2a. CBB in buck mode: $D_3=1$, $D_4=0$
Switching state during $T \cdot D_1$, where $T=1/f_{PWM}$

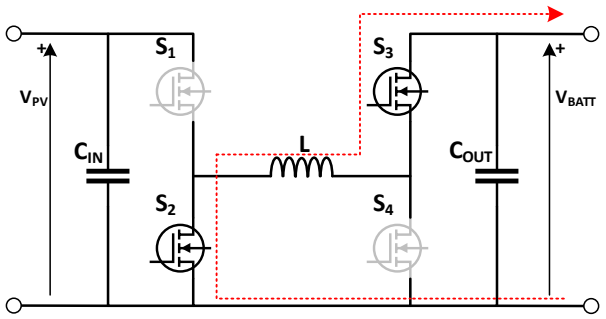

Fig. 2b. CBB in buck mode: $D_3=1$, $D_4=0$
Switching state during $T \cdot (1-D_1)$, where $T=1/f_{PWM}$

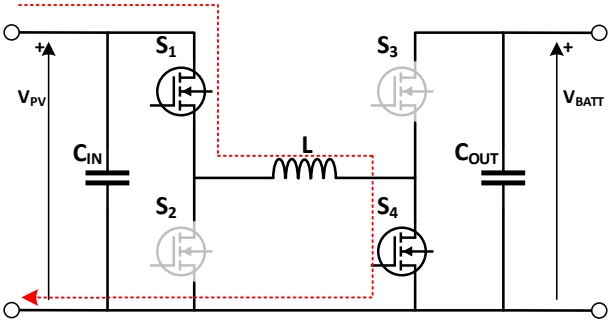

Fig. 2c. CBB in boost mode: $D_1=1$, $D_2=0$
Switching state during $T \cdot D_4$, where $T=1/f_{PWM}$

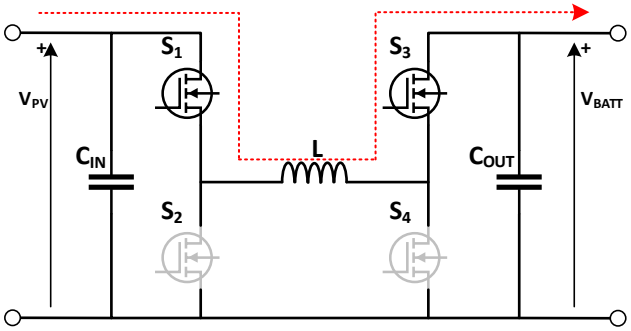

Fig. 2d. CBB in boost mode: $D_1=1$, $D_2=0$
Switching state during $T \cdot (1-D_4)$, where $T=1/f_{PWM}$

At this point, it is of great importance to conduct following discussion. For a given battery voltage (which depends on the state of battery charge) and predefined value of charging current, algorithm is realized to compute such a value of duty cycle which will provide adequate operating point on current-voltage

characteristic of PV panel in order to meet set of equations (1) or (2).

Hysteresis control is implemented. Algorithms within "CC mode" and "CV mode" blocks in Fig. 3 are basically the same. Battery current is maintained on predefined value which is $I_{LIMIT}=CC_{LIMIT}$ in case of CC mode and $I_{LIMIT}=(0.15\text{-}0.25)\cdot CC_{LIMIT}$ in case of CV mode. Simple algorithm flowchart for CC mode and CV mode is shown in Fig. 4.

In previous figure, D_X stands for duty cycle D_1 or D_4 depending on which one of buck or boost mode is active. Constants I_{LIMIT}^{+} and I_{LIMIT}^{-} are defined in (3) and they are used because of the nature of hysteresis control:

$$I_{LIMIT}^{+} = I_{LIMIT} + \Delta I_{LIMIT}$$
$$I_{LIMIT}^{-} = I_{LIMIT} - \Delta I_{LIMIT}. \quad (3)$$

Value of constant ΔI_{LIMIT} should be determined in accordance to the algorithm's best performance.

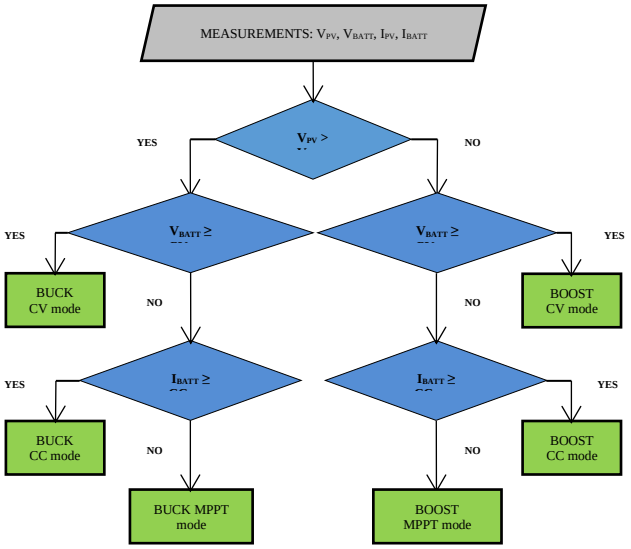

Fig. 3. General algorithm flowchart

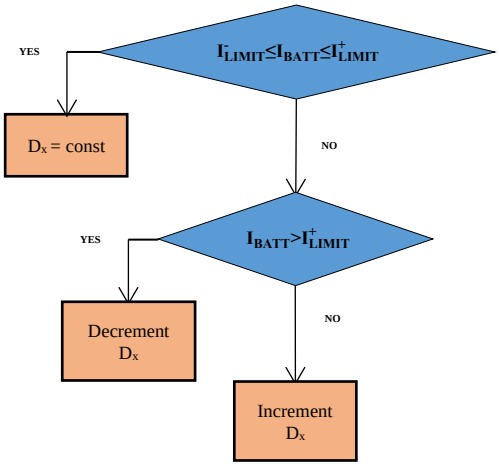

Fig. 4. Algorithm flowchart for CC and CV mode

If battery current value is within hysteresis limits, current value of duty cycle remains unchanged. If battery current value is over upper hysteresis limit, current value of duty cycle should be decremented in order to decrease battery current and put it back within the limits. If battery current value is under lower hysteresis limit, current value of duty cycle should be incremented in order to increase battery current and put it back within the limits.

Algorithm within "MPPT mode" blocks in Fig. 3 is well known Perturb & Observe (P&O) algorithm and its flowchart is shown in Fig. 5. Variable ΔP represents the difference between two consecutive PV panel power values. PV panel power is calculated as

$$P_{PV} = I_{PV} \cdot V_{PV}. \quad (4)$$

Variable ΔV represents the difference between two consecutive PV panel voltage values. Here, as well as in Fig. 4, D_X designates duty cycle D_1 or D_4, depending on which one of buck or boost mode is active. Namely, depending on signs of ΔP and ΔV it is possible to locate operating point in relation to the point of maximum power. A small shift of operating point should be enough to determine its position in relation to the maximum power point. For example, the operating point will be on the left side of the maximum power point if ΔP and ΔV both have positive or negative values after applied mentioned shift. If it is that ΔP and ΔV do not have the same sigh of value, it means that the operating point is on the right side of maximum power point. So, based on whether ΔP and ΔV are positive or negative, by changing the value of duty cycle, it is possible to reach maximum power point on current-voltage characteristic (power-voltage characteristic) of PV panel, thus providing maximum efficiency. In Fig. 6 current-voltage (I-V) and power-voltage (P-V) characteristics of PV panel are shown. For battery charging applications MPPT mode is active only if PV panel current at maximum power point provides battery current that is below current limit.

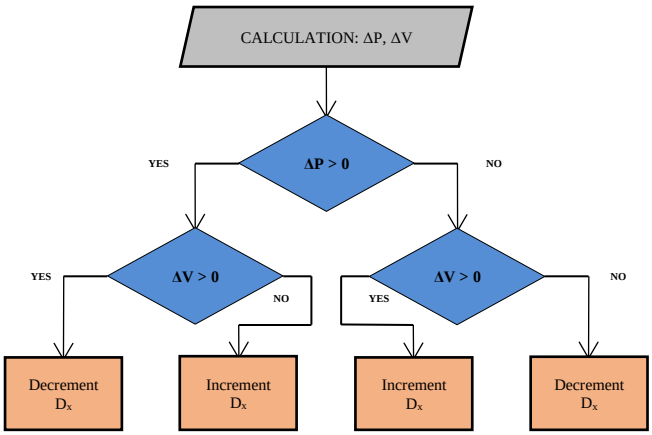

Fig. 5. Algorithm flowchart for MPPT mode

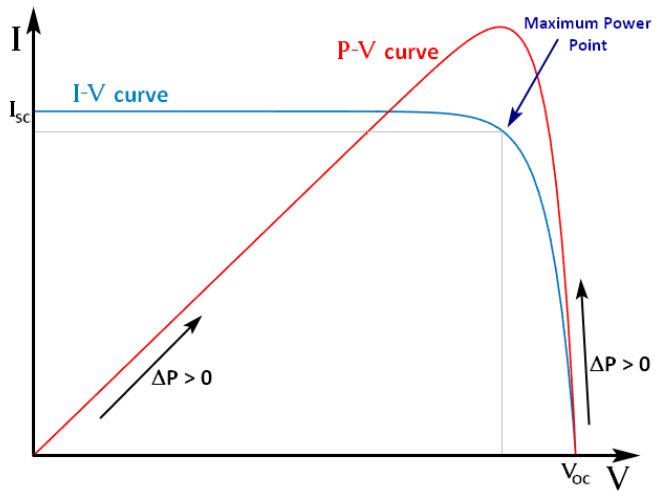

Fig. 6. I-V and P-V characteristic of PV panel

IV. HIL TEST RESULTS

The HIL laboratory setup presented in Fig. 7 consists of Typhoon HIL 602+ device [9], laptop computer and Texas Instruments TMS320F28335 microcontroller. Developed algorithm, which is previously described, is implemented on Texas Instruments TMS320F28335 microcontroller. Connections between Typhoon HIL 602+ device and microcontroller imply current and voltage measurements connections from HIL device to ADC terminals of microcontroller, as well as digital signal connections from microcontroller to HIL device. Digital signals are turn on and off commands for CBB switches. Algorithm takes into consideration dead time period of 1μs. Operation between HIL 602+ device and microcontroller is coordinated from laptop computer (Fig. 7). After starting the simulation from HIL SCADA in Typhoon HIL software, to make battery charging possible, Enable signal is required. That signal actually enables switches to operate, thus providing connection between PV panel and battery over CBB. Before Enable signal is sent, CBB is inactive. Enable signal is additional digital connection from microcontroller to HIL device and it is manipulated via laptop computer. The chosen electrical components values presented in Fig. 1 are: C_{IN}=100μF, L=500μH and C_{OUT}=150μF.

Switching frequency of MOSFET switches is f_{PWM}=50kHz. Used battery nominal voltage is 21.6V and its capacity is 3.12Ah. For CC mode current limit I_{LIMIT} is 3.1A and ΔI_{LIMIT} is 0.05A. For CV mode current limit I_{LIMIT} is 0.75A and ΔI_{LIMIT} is 0.05A. Voltage limit CV_{LIMIT} is 25V.

Different types of PV panels and different weather conditions are simulated by normalized I-V characteristics within Typhoon HIL software. Short circuit current (I_{SC}) is from a range of 0A to 10A with a step of 1A, where 0A represent the case in which there is no irradiation at all and 10A represent the case in which there is high irradiation for one particular PV panel type. Open circuit voltage (V_{OC}) is from a range of 10V to 50V with a step of 1V, where 10V could represent extremely high temperature and 50V could represent extremely low temperature for one particular PV panel type. From another point of view, if it is assumed that Standard Test Conditions for PV panels (irradiance of 1000W/m^2 and temperature of 25ºC) are met, each pair of values (I_{SC},V_{OC}) within aforementioned ranges could be viewed as specification from manufacturer for particular type of PV panel. Which one of two points of view is more appropriate to be accepted, is on the reader to decide.

There are 6 different operating modes that are investigated at the HIL laboratory setup: buck CV mode, buck CC mode, buck MPPT mode, boost CV mode, boost CC mode and boost MPPT mode. Which of operating modes should be the active one, depends on value of PV panel current I_{PV}, value of PV panel voltage V_{PV} and battery state of charge (discharge) which determines battery voltage level (Fig. 8).

The following figures present results of real time simulations obtained on previously shown experimental setup and they are captured within HIL SCADA. For each charging mode waveform of battery current is shown. Enable signal is sent at 0.3s of simulation and after transient period battery current reaches its steady-state waveform. In order to test each charging mode different initial conditions of simulations are required for each mode. For example in Fig. 9 value of V_{OC} is 32V and initial state of charge (SOC) is 99% (99% charged is equal as 1% discharged). According to Fig. 8 SOC=99% means that battery voltage is over CV_{LIMIT}. Considering general algorithm flowchart, in Fig. 9 conditions $V_{PV} > V_{BATT}$ and $V_{BATT} \geq CV_{LIMIT}$ are met and operating mode is buck CV mode.

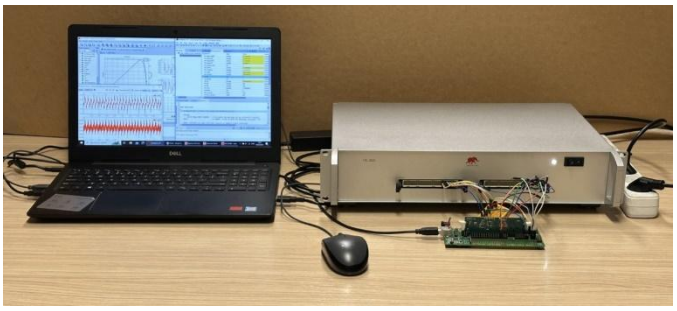

Fig. 7. Experimental setup: laptop computer, Typhoon HIL 602+ device and Texas Instruments TMS320F28335 microcontroller

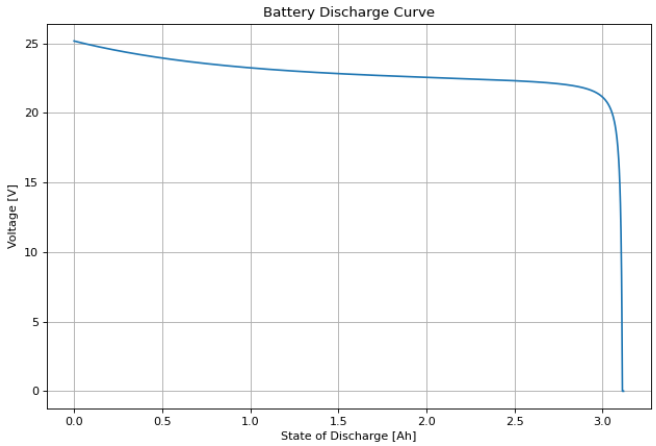

Fig. 8. Used battery discharge curve from Typhoon HIL software

Fig. 10 presents CC buck mode. Open circuit voltage is 39V, so V_{PV} is greater than V_{BATT} which means that one of buck modes should be active. Initial condition SOC=52%, according to Fig. 8, means that battery voltage is bellow CV_{LIMIT} which eliminates CV buck mode. According to set of equations (1) in buck mode PV current is lower or equal than battery current (D≤1). With short circuit current I_{SC}=8A, battery current is definitely greater

than CC_{LIMIT}. Considering general algorithm flowchart, in Fig. 10 conditions $V_{PV} > V_{BATT}$ and $I_{BATT} \geq CC_{LIMIT}$ are met and operating mode is buck CC mode.

In Fig. 11 V_{OC}=47V means that one of buck modes should be active and with SOC=68% CV buck mode is eliminated. With I_{SC}=1A battery current at maximum power point is bellow CC_{LIMIT}. Considering general algorithm flowchart, in Fig. 11 conditions $V_{PV} > V_{BATT}$ and $I_{BATT} < CC_{LIMIT}$ are met and operating mode is buck MPPT mode.

In Fig. 12 according to V_{OC} and SOC values, it can be concluded that boost CV mode should be active one. In Fig. 13 high I_{SC} value and low V_{OC} value indicate boost CC mode and in Fig. 14 low I_{SC} and low V_{OC} values indicate boost MPPT mode.

Based on figures 9 to 14 it could be stated that developed algorithm provides charging at any state of battery charge under different weather conditions (different I_{SC} and V_{OC}).

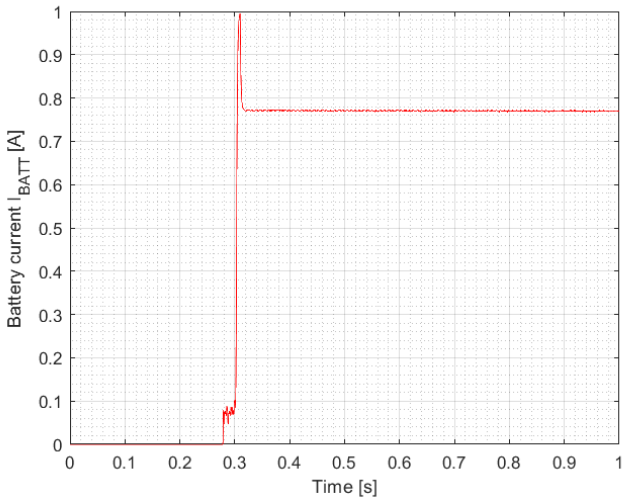

Fig. 9. Battery current in CV buck mode
Simulation initial conditions: SOC=99%, I_{SC}=5A, V_{OC}=32V

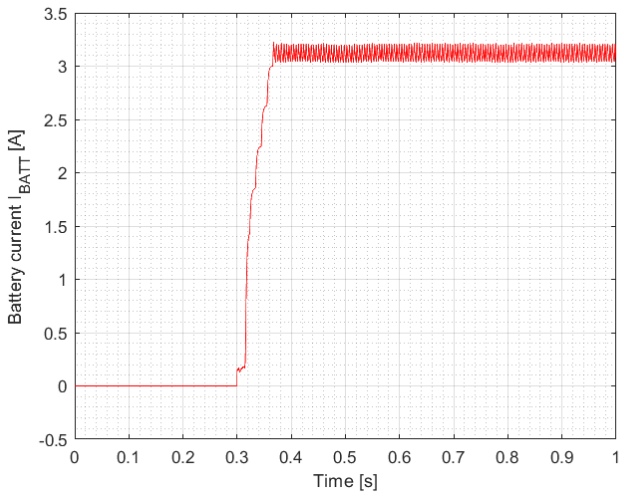

Fig. 10. Battery current in CC buck mode
Simulation initial conditions: SOC=52%, I_{SC}=8A, V_{OC}=39V

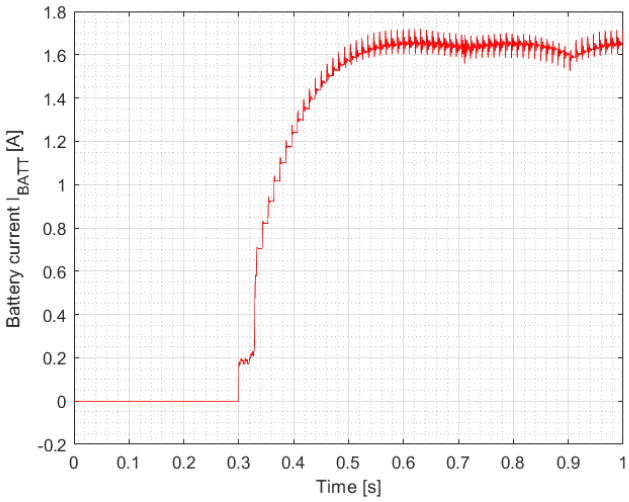

Fig. 11. Battery current in MPPT buck mode
Simulation initial conditions: SOC=68%, I_{SC}=1A, V_{OC}=47V

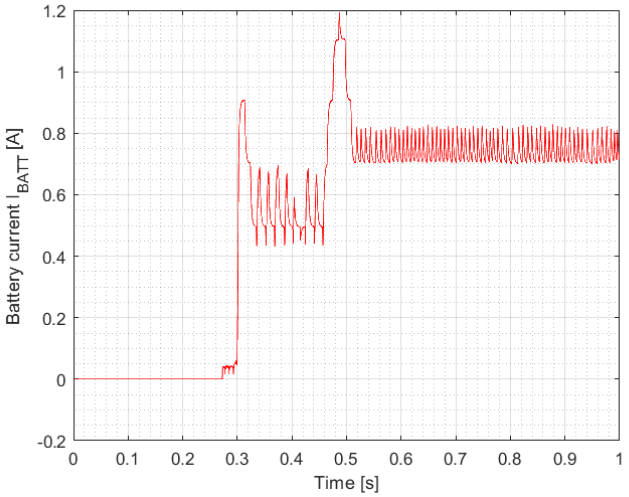

Fig. 12. Battery current in CV boost mode
Simulation initial conditions: SOC=98%, I_{SC}=7A, V_{OC}=22V

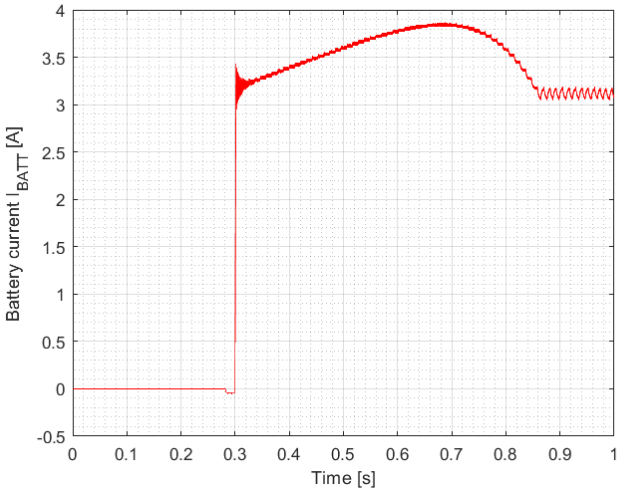

Fig. 13. Battery current in CC boost mode
Simulation initial conditions: SOC=36%, I_{SC}=9A, V_{OC}=12V

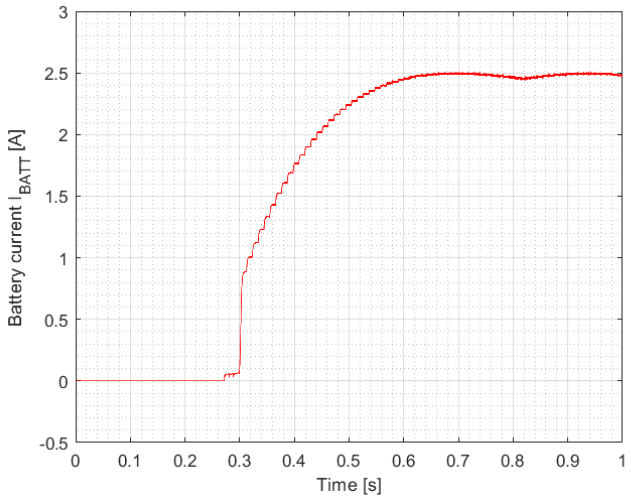

Fig. 14. Battery current and battery voltage in MPPT boost mode
Simulation initial conditions: SOC=73%, I_{SC}=4A, V_{OC}=18V

Fig. 15 shows transition from CC buck mode to MPPT buck mode due to lack of irradiation, as a result of, for example, presence of clouds. Lack of irradiation is simulated with sudden change of I_{SC} from 9A to 2A under V_{OC}=37V. Initial state of charge was 68%.

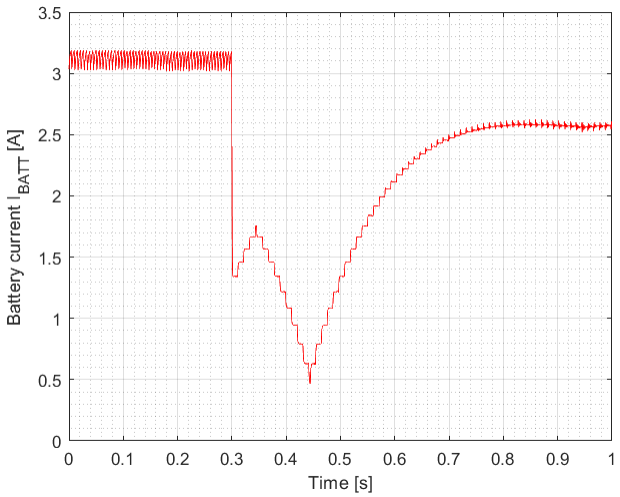

Fig. 15. Battery current for transition from CC buck mode to MPPT buck mode

V. Conclusion

Discussion above shows that is possible to construct solar charger which is operational for wide range of input voltages, even with simple control such as hysteresis control. Based on the presented results of HIL simulations, it can be concluded that each of operating modes in its steady-state controls the current value around predefined current limits with maximum current ripple around 0.1A. It can also be stated that transition between two modes (within buck modes or boost modes separately) does not endangers the battery. But, when it comes to transition from buck mode to boost mode and vice versa, simple control algorithm shown in the paper could be potentially problematic in the case of sudden and extreme changes of V_{OC} which are practically impossible in reality owing to gradual change of ambient temperature. Neglecting that, it is on safety side to predict such changes. In order to overcome potential high currents in buck-boost transitions, as a plan for future work, algorithm could be upgraded with queries for smooth transitions which would certainly have a negative effect on algorithms complexity, but positive to its robustness.

Acknowledgment

This work has been supported by the European Union's HORIZON – WIDERA – 2021 – ACCESS – 03 under grant agreement No 101079200 (SUNRISE). The authors also wish to thank Typhoon HIL for their support which made this work possible.

References

[1] Görkem ÖZKUR, Hüseyin YEŞİLYURT, "Isolated MPPT, CC, CV Solar Battery Charger Design and Application", Journal of Science and Technology 2023, 16(1), 76-88, Pages 76-88.

[2] Deepak Ravi, Shimi Sudha Letha, Paulson Samuel, Bandi Mallikarjuna Reddy, "An Overview of Various DC-DC Converter Techniques used for Fuel Cell based Applications", 2018 International Conference on Power Energy, Environment and Intelligent Control (PEEIC), Pages 16-21

[3] Jovan Mikulović, Željko Đurišić, "Solar power engineering", Academic Mind, Belgrade, 2019. (in Serbian)

[4] Linear Technology, "DEMO MANUAL DC2069A Description LT8490 High Efficiency MPPT Battery Charger Controller", 2004.

[5] Linear Technology, "High Voltage, High Current Buck-Boost Battery Charge Controller with Maximum Power Point Tracking (MPPT)", 2014.

[6] Enes Ugur, Serkan Dusmez, Bulent Vural, Mehmet Uzunoglu, "Implementation of a Reliable Load Sharing Strategy between Battery and Ultra-capacitor on a Prototype Electric Vehicle", Transportation Electrification Conference and Expo (ITEC), June 2012

[7] Noass Kunstbergs, Hartmut Hinz, Nigel Schofield, Dennis Roll, "Efficiency Improvement of a Cascaded Buck and Boost Converter for Fuel Cell Hybrid Vehicles with Overlapping Input and Output Voltages", Inventions 2022, 7, 74

[8] Miloš R. Nedeljković, Srđan L. Srdić, "Power Converters 1: Basic topologies", University of Belgrade, Faculty of Electrical Engineering, Belgrade, 2016. (in Serbian)

[9] Typhoon HIL Software manual

[10] Miguel Fernandez, Alberto Rodriguez, Miguel Rodríguez, Aitor Vazquez, Pablo Fernandez, Manuel Arias, "Smooth-Transition Simple Digital PWM Modulator for Four-Switch Buck-Boost Converters", Electronics 2022, 11, 100